Egyptian Journal of Aquatic Biology & Fisheries
Zoology Department, Faculty of Science,
Ain Shams University, Cairo, Egypt.
ISSN 1110 – 6131
Vol. 29(5): 2357 – 2372 (2025)
www.ejabf.journals.ekb.eg

Removal of Copper ions from Aqueous Solutions Using Chitosan Coated with Iron Oxide Nanoparticle

Nadia khalaf Mohsen[1], Muayad H. M. Albehadili[2], Ahmed Yousif Hammood[1]*

[1]Marine Science Center, University of Basrah, Basrah, Iraq

[2]College of Marine Science, University of Basrah, Basrah, Iraq

***Corresponding Author: ahmed.hammood@uobasrah.edu.iq**

ARTICLE INFO

Article History:
Received: July 15, 2025
Accepted: Sep. 17, 2025
Online: Oct. 11, 2025

Keywords:
Adsorption,
Chitosan/iron oxide,
Cu(II)ions,
Thermodynamics

ABSTRACT

Water samples were collected from three different locations in Basra Governorate, southern Iraq: the first from Ras Al-Bisha Al-Faw; the second from the Basra Shatt site near the main outlet of the Hamdan wastewater treatment plant, and the third from the Khor Al-Zubair site near the mangrove nursery. The prepared composite was tested as a surface that adsorbs Cu^{2+} ions from watery liquids. FT-IR, XRD, FE-SEM EDX, and zeta potential were among the methods used to characterize the produced nanocomposite. The results showed that the copper removal efficiency of the prepared surface reached 93.33% in the first location, 70.99% in the second location, and 74.02% in the third location. This study addressed the preparation of chitosan coated with nano-iron oxide. The experimental adsorption data were subjected to the Langmuir and Freundlich model mathematical equations, which took temperature study results into consideration. The particle size calculated from the Debye-Scherr equation was about 23.28nm, which was extracted from the patterns of X-ray diffraction. The purity of the phase was demonstrated, and the Langmuir equation showed a higher linear correlation than the Freundlich equation. The positive values of ΔH calculated from the thermodynamic curves demonstrated that the adhesion of copper ions was endothermic, while the negative values of ΔG confirmed the spontaneity of the adsorption process, and the positive values of ΔS indicated an increase in randomness at the solid–solution interface during adsorption.

INTRODUCTION

Over the past century, the world has witnessed rapid increase in urbanization and industrialization, resulting in the release of large quantities of heavy metal ions into the environment through various human actions, including electroplating, chemical manufacturing, mining, fertilizer use, and pesticide use **(Wai *et al.*, 2017; Hama Aziz *et al.*, 2023)**. This has transformed soil and water pollution with heavy metals into a serious global environmental and health problem **(Aldoghachi & Altamimi, 2021; Kanwal *et al.*, 2024)**. These metals are characterized by their high toxicity when exceeding

permissible limits, in addition to their persistence and not-biodegradability, like lead (II), cadmium (II), copper (II), chromium (VI), and mercury (II). These metals accumulate in watery life microbes and plants and are then spread via the food chain to humans, causing serious health problems **(Shallary *et al.*, 1998; Jumaa *et al.*, 2016; Abed *et al.*, 2025)**. For example, copper (Cu^{2+}) is an essential element in biological reactions at low concentrations, but it becomes toxic when accumulated in the environment, disrupting enzyme activity, causing oxidative stress, and negatively impacting liver, kidney, and nervous system function **(Zhao *et al.*, 2008; Cui *et al.*, 2009; Li *et al.*, 2009)**.

Given these risks, there is an urgent need to develop effective technologies to remove copper ions from contaminated water. Although several conventional methods exist to address this problem, such as electrochemical treatment **(Bartosch *et al.*, 2001)**, chemical precipitation **(De vries *et al.*, 2008)**, membrane filtration **(Cheng *et al.*, 2019)**, and ion exchange **(Ibrahim *et al.*, 2020; Alhamadany *et al.*, 2021)**, these methods often suffer from limitations related to efficiency, cost, and operational complexity. In contrast, adsorption is one of the most widely used methods due to its simplicity, effectiveness, and low cost **(Foo & Hameed, 2009; Crini & lichtfouse, 2019; Cai *et al.*, 2022)**. In this context, chitosan-coated iron oxide nanoparticles (CS-Fe_3O_4) have gained increasing attention in recent years as promising adsorbents for water treatment **(Mukherjee, 2006; Liangrong, 2010; Sweesy & Elazab, 2017)**. Chitosan is characterized by its abundance of amine and hydroxyl groups, which provide effective binding sites for heavy metal ions, while the iron oxide particles impart magnetic properties that enable the adsorbent to be easily recovered from solutions using an external magnetic field **(Crini & Badot, 2008; Zargar *et al.*, 2015; La- Casas, 2023)**. This integration between chitosan and iron oxide enhances the copper removal efficiency and enables highly efficient reuse of the adsorbent.

Several studies have also demonstrated the success of CS-Fe_3O_4 nanocomposites in removing toxic metals, including copper, from aqueous solutions **(Allan *et al.*, 1984; Onsoyen & Skaugrud, 1990; Kurita, 1998; Lu *et al.*, 2001; Evans *et al.*, 2002)**. The preparation method is a key factor in determining the physicochemical properties of these materials, with techniques such as co-precipitation or sol-gel methods being used, while surface coating with chitosan reduces agglomeration and increases stability **(Agnihotri *et al.*, 2004; Des Rieux *et al.*, 2006; Grenha *et al.*, 2010)** In addition, green methods based on plant extracts rich in organic acids (such as lemon juice containing citric acid) have emerged as an environmentally friendly and cost-effective option for the production of the nanomaterials.

The goal of this work was to use adsorption to extract copper, a common hazardous metal, from aqueous solutions. In order to help provide efficient solutions for treating this, the synthesized compound was used as an adsorbent surface to confirm its effectiveness in adsorbing copper ions from contaminated water.

MATERIALS AND METHODS

1. Chitosan extraction from shrimp shells

Shrimp shells were separated and thoroughly washed with tap water to remove the remaining fleshy part according to the method of **Toan (2009)**. They were then placed in mesh containers to remove excess water. Demineralization was carried out by treating the shells with a 1N hydrochloric acid solution at room temperature for 16h at a weight-to-volume ratio of 5:11. The shells were then washed with water until pH 7 was reached. Deproteinization was carried out using a 1N sodium hydroxide solution for 2h at 65°C at a weight-to-volume ratio of 10:1. The shells were then thoroughly washed with distilled water several times. Finally, the resulting product (chitin) was washed with distilled water and dried at 65°C for 24h. Chitosan was prepared by deacetylation, by treating dried chitin with a 50% sodium hydroxide solution at a temperature of 100°C for 5- 6h at a ratio of 15:1 weight to volume. It was washed with deionized water several times to reach pH 7 and was then dried at a temperature of 65°C for 24h **(Shahidi & Synowiecki, 1991; Al-dubakel *et al*., 2018)**.

2. Coating iron oxide nanoparticles with chitosan (Cs-Fe_3O_4)

1g of chitosan was dissolved in a solution consisting of 4mL of glacial acetic acid and 200mL of deionized water. The solution was stirred at 40°C until the chitosan dissolved. 1g of iron oxide (96%; Aldrich) nanoparticles was then added and left under mechanical stirring for 30min, followed by ultrasonic irradiation (225mL) of 1M sodium hydroxide. 98.9% Merck was then added, resulting in the formation of a brownish-black precipitate. The precipitate was washed several times with deionized water until the pH was equalized. The precipitate was separated using a magnet and dried for 3h at 50°C.

3. Characterization techniques

A variety of advanced and highly efficient analytical techniques were used in this study for diagnostic purposes. These techniques included infrared Fourier transform (FTIR) X-ray spectroscopy (SHIMADZU, Japan), diffraction (XRD) field emission scanning electron microscopy (FESEM) (PANalytical, UK), (TESCAN, X-rayenergy dispersive Czech Republic), spectroscopy (EDX) (TESCAN,The Czech Republic), and zeta potential. In addition, copper (II) ion concentrations were measured using atomic absorption from flames spectrometry (FAAS) (PG instruments AA500, UK).

4. Adsorption studies

By dissolving 0.380g of $Cu(NO_3)_2.4H_2O$ (99.8% Merck) in 1000mL of distilled deionized water, standard solutions for Cu (II) ions at concentrations of 1000mg/ L were created. For this investigation, range of remedies were then prepared to suit the sensitivity of the flame atomic absorption spectrometry (FAAS) spectrometer used, with concentrations of Cu (II) ions ranging from 40- 70mg/ L. To determine the optimal pH, buffer solutions with pH ranges of 3- 9 were used. The time required to reach equilibrium on the prepared nanocomposite surface was investigated over various eras, ranging from

5- 180mi at 25°C. The first volumes and concentrations of Cu (II) ions were 50mg/L and 25mL, using a constant weight of 0.02g of adsorbent. The conical flasks were set up at 120rpm in a shaking incubator. Equations 1 and 2 were used to determine the adsorption capacity (Qe) and adsorption ratio (R%) (**Hu *et al.*, 2013):**

$R\% = [(C_o - C_e)/C_o] \times 100$…….(1)

$Q_e = V(C_o - C_e)/m$ …….(2)

Where, m is the adsorbents wight (g), V is the solutions volume(L), C_o is the starting adsorbent concentration (mgL^{-1}), C_e is the remaining adsorbent concentration and Q_e is the adsorption capacity (mg/g).

5. Thermodynamic coefficients

Different concentrations of copper (II) ions (40-70 mgL^{-1}) were prepared. The samples were then put into flasks, and 0.02g of iron-coated chitosan was added to them. The flasks were set up at 120rpm in a shaking incubator at different temperatures (10.0, 25.0, 37.5, and 50.0°C). The copper (II) ions concentrations were computed. The quantities of free energy (ΔG), enthalpy (ΔH), and entropy (ΔS) were determined using equations (3-5)

$\Delta G = -RT \ln k$……..(3)

$K = C_{solid} / C_{liquid}$……(4)

$\ln K = \Delta S / R - \Delta H / RT$….. (5)

Where, K is the equilibrium constant and ΔG is the Gibbs free energy ($kJ.mol^{-1}$), Csolid is the equilibrium concentration in the solid phase (mgL^{-1}), Cliquid is the concentration in the liquid phase at equilibrium (mgL^{-1}), R is the gas constant and T is the solution temperature in Kelvin, and (0.0083 $kJ.K^{-1}$ mol^{-1}). Equation (5) was utilized to extract the slope and intercept values in order to determine ΔS ($kJ.mol^{-1}$) and ΔH ($kJ.mol^{-1}$).

6. Surface activation method of adsorbent

To study the recovery of copper (II) ions from the surface of the aqueous material, the volume and concentration of copper (II) were measured (50mg/L, 25ml), Additionally, conical flasks containing 0.02g of adsorbent were then positioned in a shaking incubator set to 120rpm, 25°C and 60min for reaching equilibrium magnetic field. Then, 25ml of hydrochloric acid with a concentration of 0.5 N was then used to extract. The adsorbent surfaces were supplemented with saturated Cu (II) ions. The shaking procedure was done for a suitable period of time. Following that, the adsorbent was removed by filtration, and the ion concentrations in the filtrate were measured using atomic absorption spectroscopy, thus determining the concentration of Cu (II) ions extracted from the surface of the adsorbent.

Equation (6) was used to obtain the recovery percentage (S%) **(Zhang & Hu, 2003):**

$$S\% = \frac{C_d \ V_d}{Q_e \ m} \times 100 \quad \ldots\ldots\ldots\ldots(6)$$

Where:
S% is the recovery percentage
Qe is the gravimetric adsorption capacity, expressed in mg/g.
$C_d$is the solution content in (mgL^{-1}). following the grafting process
$V_d$is the washing solution 's volume in units (L).
M is the adsorbed material's weight in (g).

RESULTS AND DISCUSSION

1. Findings and conversation

Fig. (1a) shows the infrared spectra of the coated chitosan. A weak absorption band was observed at 191cm (2871nm), attributed to the stretching vibration of the aliphatic C-H group. Clear bands of the amide group also appeared in the range of 1654.61-1557.85 cm^{-1}. Additionally, bands were observed in the range of 1309.13-1427.01 cm^{-1}, attributed to the bending vibration of the H group (C-). Bands appeared in the range of 1024.16-1151.16 cm^{-1}, attributed to the stretching vibration of the C-O group. We also observed bands in the range of 1439.02-2529.86 cm^{-1}, attributed to the stretching vibrations of the Fe-O group.

Fig. (1b) shows the X-ray diffraction spectra of the coated chitosan. Clear peaks appear within the angular range (10-80=20) in the following locations:
24.50, 27.63, 33.46, 35.87, 41.23, 49.83, 54.54, 57.89, 63.17 =20°
The highest intensity peak was observed in 27.63=20°

These peaks indicate the crystalline nature of the prepared composite, and were found to be consistent with the standard card (JCPDS file No.: 22-1012). These results are also consistent with the study of Bharathi and his group **(Pérez *et al*., 2019)**. The sizes of the crystals in the prepared compounds were determined using the Debye-Scherrer equation **(Cullity & Stock, 2001; AlKatrani *et al*., 2018)** (Fig. 2), based on the peak width at mid-intensity (FWHM) of the highest peak in the XRD spectrum. The results showed that the prepared compound was characterized by crystal size purity and a particle size of 23.28nm.

Fig. (1c) shows scanning electron microscope images of a nano chitosan-coated composite, showing quasi-spherical particle patterns. The images also revealed clear agglomerations in the surface structure, in addition to the presence of pores or holes on the surface of the composite. The results of the image analysis evealed that the prepared composite possessed crystalline sizes are in the nanoscale range. To accurately determine the particle dimensions, Image-J software, a powerful image analysis and particle size measurement tool, was used. The analysis results showed that the average particle dimensions reflect the structural composition of the composite material. In the case of encapsulated chitosan, the granular characteristics were accurately determined, with particle sizes ranging from 13.587 to 46.196nm, with an average of 25.917nm. This granular distribution reflects the medium to high specific surface area of the material,

which enhances its adsorption efficiency. The smaller the particle size, the greater the surface area available for the interaction of ions or molecules with surface active sites, making encapsulated chitosan an effective material for removing contaminants from aqueous solutions and treating industrial water.

The energy-dispersive X-ray (EDX) spectrum of the composite (encapsulated chitosan) shows three distinct energy peaks at 0.7 keV and 0.5 keV, as well as two additional peaks at 6.4 keV and 7.1 keV, which are attributed to iron. Among these, one peak is highly intense, while the other two exhibit lower intensities (Fig. 1d). An energy peak at 0.27 kev is attributed to carbon, another peak at 0.24 kev indicates the presence of nitrogen, and an energy peak at 0.52 kev is attributed to oxygen.

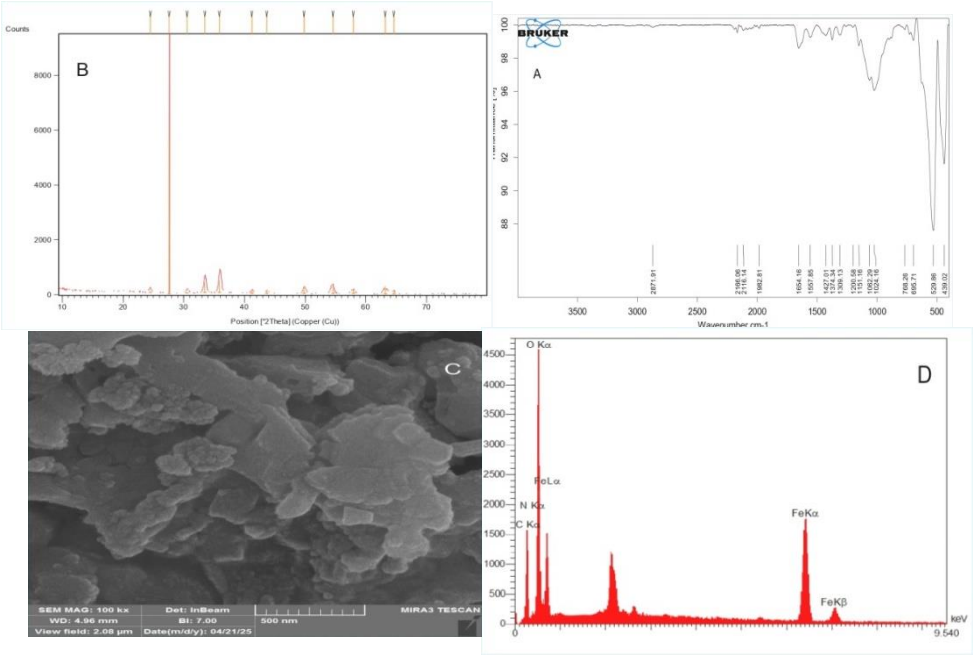

Fig. 1. The chitosan-based nanocomposite's (a) FT-IR spectra, (b) XRD spectrum, (c) FESEM images and (d) EDX spectra

2. Zeta potential

The zeta potential is an important indicator of the surface charge and physical stability of colloidal particles, as electrostatic repulsion between particles with similar charges prevents their aggregation. It is believed that good stability of colloids is achieved at positive or negative surface potential values greater than ±30 mV. Values ±30 mV or less may lead to the colloidal material's physical instability system. The results of measuring the zeta potential of the iron-coated chitosan composite showed a value of -30.7 mV, indicating that the particles have a good degree of stability in aqueous solutions, as shown in Fig. (2) **(Honary & Zhair, 2013; Labied *et al.*, 2018)**.

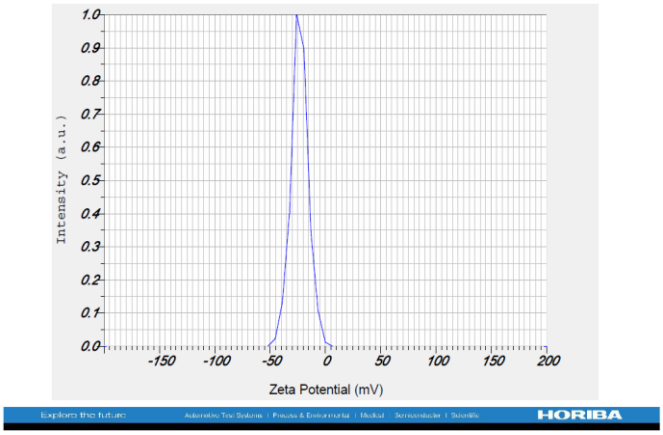

Fig. 2. Zeta potential

3. Adsorption research

3.1. Effect time of contact

Equilibrium time's impact on the adsorption of copper Cu (II) ions was studied over time periods of 5 to 180min at 25°C. Fig. (3) findings demonstrated that the adsorption method reached the equilibrium Cu (II) time at 60 min. The removal rate of Cu (II) was found to be 64.42%. We observed a significant increase in the removal rate values during the adsorption process's initial minutes, followed by a decrease in the increase up to saturation was reached, indicating that the active sites on the prepared material's surface were fully occupied and bound to the adsorbed ions **(Bumajdad & Hasila, 2023)**.

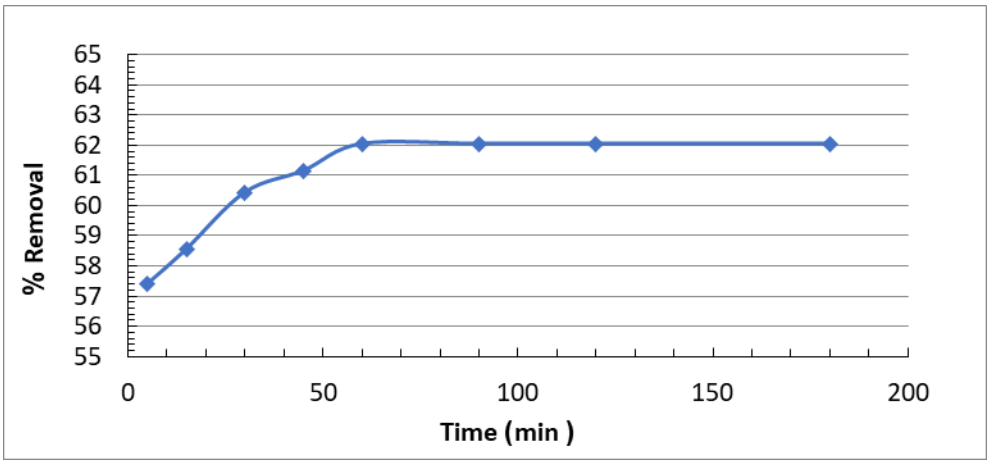

Fig. 3. Equilibrium time curves for Cu(II).

3.2. Effect of pH

Changing the pH of a solution is a key factor in determining the amount of adsorbed material, which can lead to an increase, decrease, or stabilization of copper adsorption. This process depends primarily on the nature of the solvent, the adsorbing surface's characteristics, and the chemical condition of the adsorbed ions. In this study, the effect

of pH on the adsorption of Cu (II) ions using a nanocomposite of chitosan coated with nano-iron oxide was evaluated at pH values 3, 5, 7, and 9. The initial concentration was constant and the equilibrium time was 60min at 25°C. Fig. (4) shows that the adsorption process is affected by pH. The results showed that the basic medium was more efficient at removing Cu (II) ions compared to the acidic medium **(Cheng, 2014; Yahya *et al.*, 2020)**. At acidic values, the active sites are exposed to an increased concentration of hydrogen ions (H+), which leads to their positive charge and consequently their repulsion with positive copper ions. Conversely, at higher pH values, the active sites lose their protons, allowing a greater number of active groups to bind to metal ions. Furthermore, higher pH increases the number of cationic binding sites and, at the same time, leads to a decrease in the solubility of Cu (II) ions, which enhances the adsorption efficiency on the surface of the chitosan-coated iron nanocomposite. Cu (II) removal was performed at pH=5.53 in all experiments to ensure that the adsorption and deposition processes did not interfere with each other **(An, 2020)**.

The results showed that the rate of Cu (II) ion removal increased in basic media compared to acidic media. This is attributed to the positive charge of the active sites, which leads to repulsion between them and positive copper ions, thus reducing the adsorption efficiency. High pH value removes protons from active sites, allowing copper ions to be present at those sites on the surface of the adsorbent. To prevent any interference between the adsorption and deposition processes, pH=5.53 was adopted in this study.

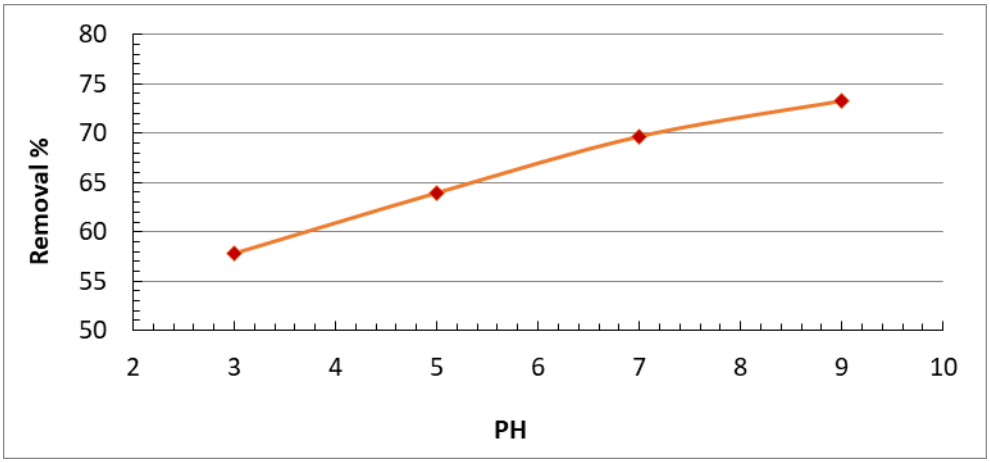

Fig. 4. Effect of pH on Cu (II).

3.3. Adsorption isotherm

Four temperatures (10, 25, 37, and 50°C) were used to study the adsorption equation, as shown in Fig. (5). The isotherm is classified as type (H), indicating adsorption characterized by a high affinity for ions, which can be observed even in highly dilute solutions. The results also showed that the amount of copper ions adsorbed on the studied surface increases with increasing initial concentrations of these ions. This is attributed to

the electrostatic attraction between copper(II) ions and the active sites on the surfaces of the adsorbent materials **(Mendizabal *et al.*, 2024)**. It was also found that the amount of adsorbed ions increases with increasing temperature. This is consistent with adsorption being an endothermic process. Increasing temperature increases the diffusion rate of ions on the surface of the material and within its pores, making adsorption on the prepared surface more efficient at higher temperatures. To more accurately evaluate the adsorption behavior, the Langmuir-Freundlich model was used to determine how copper ions bind to the surface. Freundlich (Eq. 8) and Langmuir (Eq. 9) equations were also employed to track the results.

The following equations show the isothermal adsorption line's adsorption data:

$\log Qe = \log Kf + 1/n \log Ce$. . . . (8)

$Ce/Qe = 1/Qmb + Ce/Qm$ . . . . (9)

Where, Kf is the adsorption coefficient and n are the adsorption intensity, capacity, b is the maximum adsorption capacity (mg/g) and Qm is the adsorption energy, plots of the Freundlich equation's logQe and logCe values and the Langmuir equation's Ce/Qe and Ce values were made. The results showed higher values of the correlation value (R^2) in comparison with the Freundlich equation, as shown in Table (1) **(Adriansyah *et al.*, 2018)**. This indicates that the Langmuir equation can be used to model the adsorption of Cu (II) ions. The current results show that the process of adsorption occurred on a single layer and that the surfaces were homogeneous **(Mohammed *et al.*, 2021)** i.e., they contained sites with identical adsorption energy.

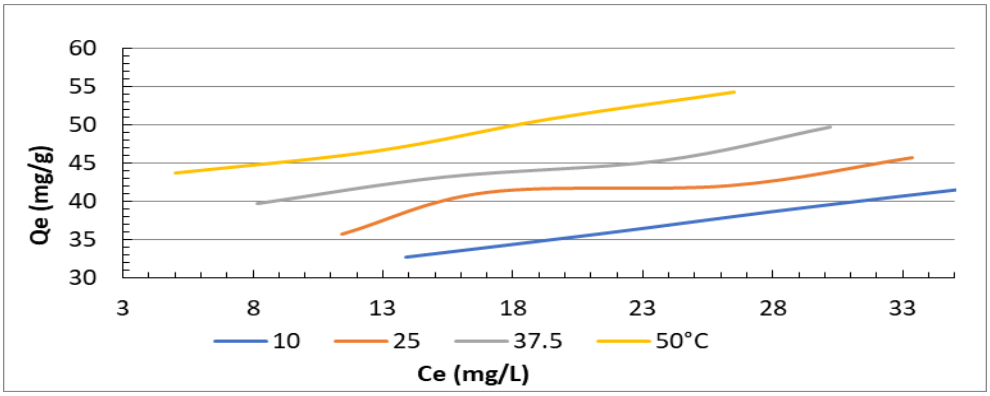

Fig. 5. Cu (II) adsorption isotherm

Table 1. Outcomes of applying Langmuir and Freundlich isotherms

Temp. (C)	Langmuir constants			Freundlich constants		
	Q_m (mg/g)	b (L/mg)	R^2	n	Kf	R^2
10.0	46.617	0.216	0.9727	4.909	19.783	0.8542
25.0	52.015	0.197	0.9932	4.818	21.945	0.9060
37.5	54.062	0.288	0.9918	6.336	28.254	0.9394
50.0	57.843	0.447	0.9938	7.883	34.9879	0.9181

3.4 The study of thermodynamics

Thermodynamic functions were calculated in this study at four temperatures (10-50°C), as shown in Table (2). A linear correlation coefficient between lnK and 1/T, was discovered (R2 = 0.9983-0.9963). Positive values of ΔH (75.18 and 137.11 kJ/mol-1) confirmed that the process of adsorption was endothermic **(Fenti *et al.*, 2020)**.

An increase in unpredictability was shown by positive values of ΔS **(Giles *et al.*, 1960)**. Values of ΔG were all negative, becoming more negative with increasing temperature, indicating the spontaneity of the process **(Kippling, 1965; Cruz-Lopes, 2021)**. The values of ΔG ranged from -22.64 to 78.71 kJ mol-1. According to what is mentioned in the literature, the adsorption is physical when the values of ΔG range from 0 to -20 kJ mol-1, while for values more negative than -40 kJ mol, the adsorption is chemical.

Table 2. Adsorption of Cu (II) ions using thermodynamic functions

Co (mg/L)	K				- ΔG				ΔH	ΔS
	Temperature									
	283	298	310.5	323	283	298	310.5	323		
40	1.883	2.499	3.889	6.984	11.90	25.41	36.67	47.937	24.05	0.900
50	1.577	1.937	2.246	2.933	9.871	16.37	21.79	27.211	112.8	0.433
60	1.082	1.280	1.530	2.099	0.591	7.020	12.37	17.734	120.7	0.428
70	0.892	1.098	1.317	1.640	3.203	2.604	7.444	12.284	112.8	0.387

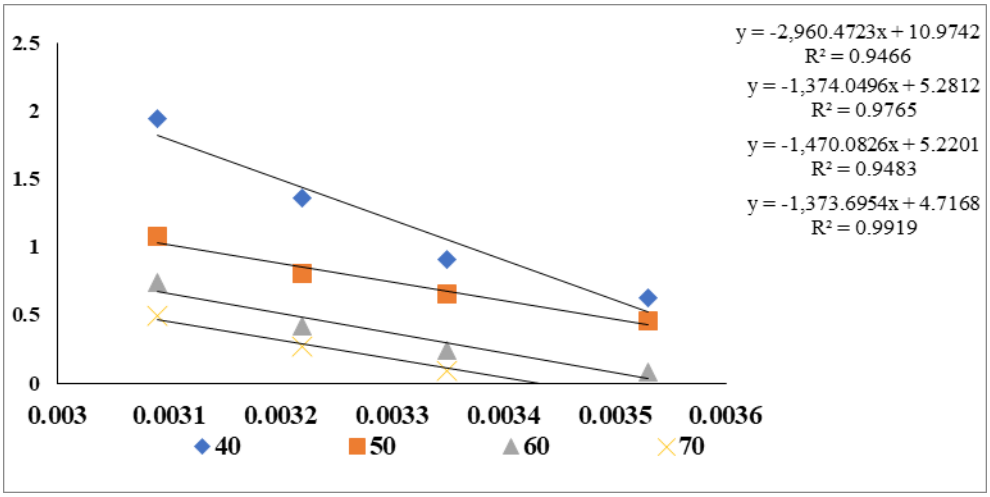

Fig. 6. Plot of lnK against 1/T for adsorption

3.5. Practical applications

The practical applications involved the use of the prepared adsorbent surfaces to remove copper ions from seawater and wastewater samples taken from three different sites: the first site in Al-Faw (Ras Al-Bisha); the second site on the Shatt Al-Basra River

near the wastewater outlet of the Hamdan Main Station of the Basra Governorate Sewerage Directorate; and the third site on the Khor Al-Zubair near the mangrove nursery. The results shown in Table (3) demonstrate the high efficiency of the prepared adsorbent surfaces in removing copper ions, with the removal percentage reaching 93.33% for the first location, 67.77% for the second location, and 62.00%for the third site **(Jin *et al.*, 2022)**. This indicates the potential for using these surfaces as effective materials for treating water contaminated with copper ions.

Table 3. Percentage removal of ions

Site	Ion	contact time (min)	pH	C_o (mg/L)	C_e (mg/L)	Q_e (mg/g)	Removal %
St_1	Cu(II)	60	8.51	0.09	0.006	0.105	93.33
St_2	Cu(II)	60	7.72	0.180	0.058	0.152	67.77
St_3	Cu(II)	60	8.35	0.050	0.019	0.038	62.00

3.6. Activate adsorbent surfaces

he recovery of Cu(II) ions from the constructed adsorbent surface was examined, given the importance of reusing the adsorbent and recovering the adsorbed ions. The results showed a high recovery rate during the first activation, reaching 90.68%. However, the recovery rate decreased during the second activation, reaching 84.82% **(Vakili *et al.*, 2019)**. These results indicate that it is possible to reuse the produced adsorbent multiple periods while preserving its efficiency in adsorbing copper ions. The decreased adsorption rate in acidic media is attributed to the increased hydrogen ion (H+) concentration at low pH, which results in competition between copper ions for the active sites on the adsorbent surface, reducing adsorption and increasing the dissociation rate.

CONCLUSION

This study addressed the preparation of iron nano-coated chitosan composite. The surface area values of the prepared composite were relatively high. The effect of various parameters, such as temperature, primary ion concentration, pH, equilibrium time, and ion concentration on the adsorption process was investigated. The equilibrium time for copper ions was maintained for 60min. The results showed 64.42% removal of copper ions. The Freundlich-Langmuir model was applied to the process and the Langmuir model was shown to be more consistent with the isotherm. The thermodynamics indicates that the adsorption process is spontaneous and endothermic. This suggests that the prepared composite could be a very effective heavy metal adsorbent for environmental protection. Experimental applications were conducted on water samples from three

different marine sites: Al-Faw (Ras Al-Bisha), the Shatt Al-Basra River near the wastewater outlet of the Hamdan Main Station, which is part of the Basra Governorate Sewerage Directorate, and the third is Khor Al-Zubair near the mangrove nursery. Table (3) shows that the prepared adsorbent surface has high efficiency in removing Cu (II) ions.

REFERENCES

Abed, J.M.; Ali, A.H.; Yaseen, A.T.; Al-Faisal, A.; Mutlak, F.; Jassim, F.K.; Jerry, Dean R. and Jawad, L.A. (2025). Barramundi (*Lates calcarifer*) from Iraq: a new record for the Arabian Gulf, with a highlight on it genetic origins and description of two skeletal deformities. New Zealand Journal of Zoology, 52(1): 40-54.

Adriansyah, R.; Restiasih, E. and Meileza, N. (2018). Biosorption of Heavy Metal Ions Cu (II) and Cr (VI) Using Xantasi Coffee Husk Biosorbent ALOTROP. J. Educ. Chem, 2, 114-121.

Agnihotri, S.A.; Mallikarjuna, N.N. and Aminabhavi, T.M. (2004). Recent advances on chitosan-based micro-and nanoparticles in drug delivery. Journal of controlled release, 100(1): 5-28.

Aldoghachi, M.A. and Altamimi, E.D. (2021). Assessment of Water Quality Using Heavy Metals Concentrations in Several Water Resources of Shatt Al-Arab and Tissues of the Nile Tilapia (*Oreochromis niloticus*) and the Shrimp (*Metapenaeus affinis*). Egyptian Journal of Aquatic Biology and Fisheries, 25(2): 803-817.

Al-Dubakel, A.; Al-Shatty, S. and Al-Noor, J. (2018). Removing of heavy metals from sewage water using chitosan extracted from crustacean waste. Syrian Journal of Agricultural Research, 5(2): 189–200.

Alhamadany, Q.H.; Yaseen, A.T.; Yasser, A.T. and Ali, A.W. (2021). Chemical and mineral composition of ten ecomonically important fish species in the Satt Al-Arab river and Iraqi marine water Northern West Arabian gulf. Iraqi Journal of Agricultural Sciences, 52(3): 632–639.

AlKatrani, L.M.; Al-Zaidy, F.M. and Aldoghachi, M.A. (2018). Effect of Sudden and Gradual Transfer of *Oreochromis aureus* to Different Water Salinities on the Activity of AST and ALT Serum Enzymes. JKAU: Mar. Sci., 28 (2): 81-88.

Allan, G.G., and Altman, L.C. (1984). Biomedical applications of chitin and chitosan. In J. P. Zikakis (Ed.), Chitin, chitosan and related enzymes (pp. 119–133). New York: Academic Press.

An, B. (2020). Cu (II) and As (V) adsorption kinetic characteristic of the multifunctional amino groups in chitosan. Processes, 8(9): 1194.

Aziz, K.H.H.; Mustafa, F.S.; Omer, K.M.; Hama, S.; Hamarawf, R.F. and Rahman, K.O. (2023). Heavy metal pollution in the aquatic environment: efficient and low-cost removal approaches to eliminate their toxicity: a review. RSC advances, 13(26): 17595-17610.

Bartosch, K. and Mersmann, A. (2001). Direct contact cooling techniques in melt suspension crystallization and their effect on the product purity. Chemical engineering science, 56(7): 2347-2356.

Bumajdad, A. and Hasila, P. (2023). Surface modification of date palm activated carbonaceous materials for heavy metal removal and CO2 adsorption. Arabian Journal of Chemistry, 16(1): 104403.

Cai, J.; Niu, B.; Xie, Q.; Lu, N.; Huang, S.; Zhao, G. and Zhao, J. (2022). Accurate removal of toxic organic pollutants from complex water matrices. Environmental Science and Technology, 56(5): 2917-2935.

Cheng, C.; Liu, Z.; Li, X.; Su, B.; Zhou, T. and Zhao, C. (2014). Graphene oxide interpenetrated polymeric composite hydrogels as highly effective adsorbents for water treatment. RSC Advances, 4(80): 42346-42357.

Cheng, X.; Liang, H.; Ding, A.; Tang, X.; Liu, B.; Zhu, X. and Li, G. (2017). Ferrous iron/peroxymonosulfate oxidation as a pretreatment for ceramic ultrafiltration membrane: Control of natural organic matter fouling and degradation of atrazine. Water Research, 113: 32-41.

Crini, G. and Badot, P.M. (2008). Application of chitosan, a natural amino polysaccharide, for dye removal from aqueous solutions by adsorption processes using batch studies: A review of recent literature. Progress in polymer science, 33(4): 399-447.

Crini, G. and Lichtfouse, E. (2019). Advantages and disadvantages of techniques used for wastewater treatment. Environmental chemistry letters, 17(1): 145-155.

Cruz-Lopes, L.P.; Macena, M.; Esteves, B. and Guiné, R.P. (2021). Ideal pH for the adsorption of metal ions Cr6+, Ni2+, Pb2+ in aqueous solution with different adsorbent materials. Open Agriculture, 6(1): 115-123.

Cui, W.; Peng, X.; Zhao, L.; Yang, F. and Cui, H.M. (2009). Effect of high copper on the antioxydic function of kidney in ducklings. Acta Veterinaria et Zootechnica Sinica, 40(4): 572-576.

Cullity, B.D. and Stock, S.R. (2001) Elements of X-ray Diffraction Third Edition,

De Vries, W.; Römkens, P.F.A.M. and Bonten, L.T.C. (2008). Spatially explicit integrated risk assessment of present soil concentrations of cadmium, lead, copper and zinc in the Netherlands. Water, Air, and Soil Pollution, 191(1): 199-215.

des Rieux, A.; Fievez, V.; Garinot, M.; Schneider, Y. J. and Préat, V. (2006). Nanoparticles as potential oral delivery systems of proteins and vaccines: a mechanistic approach. Journal of controlled release, 116(1): 1-27.

Evans, J.R.; Davids, W.G.; MacRae, J.D. and Amirbahman, A. (2002). Kinetics of cadmium uptake by chitosan-based crab shells. Water research, 36(13): 3219-3226.

Fenti, A.; Iovino, P. and Salvestrini, S. (2019). Some remarks on "A critical review of the estimation of the thermodynamic parameters on adsorption equilibria. Wrong use

of equilibrium constant in the Van't Hoff equation for calculation of thermodynamic parameters of adsorption". Journal of Molecular Liquids, 276: 529–530.

Foo, K.Y. and Hameed, B.H. (2009). Value-added utilization of oil palm ash: A superior recycling of the industrial agricultural waste. Journal of hazardous materials, 172(2-3): 523-531.

Giles, C.H. (1960). Studies in adsorption: Part X1. A system of classification of solution adsorption isotherms, and its use in diagnosis of adsorption mechanisms and in measurement of specific surface areas of solids. J. chem. Soc., 111, 3973-3993.

Grenha, A., Gomes, M.E., Rodrigues, M., Santo, V.E., Mano, J.F., Neves, N.M., and Reis, R.L. (2010). Development of new chitosan/carrageenan nanoparticles for drug delivery applications. Journal of Biomedical Materials Research Part A: An Official Journal of The Society for Biomaterials, The Japanese Society for Biomaterials, and The Australian Society for Biomaterials and the Korean Society for Biomaterials, 92(4): 1265-1272.

Honary, S. and Zahir, F. (2013). Effect of zeta potential on the properties of nano-drug delivery systems-a review (Part 2). Tropical journal of pharmaceutical research, 12(2): 265-273.

Hu, X.J.; Liu, Y.G.; Wang, H.; Chen, A.W.; Zeng, G.M.; Liu, S.M. and Liu, S.H. (2013). Removal of Cu (II) ions from aqueous solution using sulfonated magnetic graphene oxide composite. Separation and purification technology, 108: 189-195.

Ibrahim, Y.; Naddeo, V.; Banat, F. and Hasan, S.W. (2020). Preparation of novel polyvinylidene fluoride (PVDF)-Tin (IV) oxide (SnO2) ion exchange mixed matrix membranes for the removal of heavy metals from aqueous solutions. Separation and purification technology, 250: 117250.

Jin, X.; Liu, R.; Wang, H.; Han, L.; Qiu, M. and Hu, B. (2022). Functionalized porous nanoscale Fe3O4 particles supported biochar from peanut shell for Pb (II) ions removal from landscape wastewater. Environmental Science and Pollution Research, 29(25): 37159-37169.

Jumaa, Mustafa N.; Yaseen, Nahi Y.; Karim, Rafid M.; Shehab, Adil F.; Sagban, Likaa H. (2016). Study of genetic variations of FTO gene and its relationship to obese in Iraqi population. Der Pharma Chemica, 8(18): 242-254.

Kanwal, H.; Raza, A.; Zaheer, M.S.; Nadeem, M.; Ali, H.H.; Manoharadas, S. and Rasool, F. (2024). Transformation of heavy metals from contaminated water to soil, fodder and animals. Scientific Reports, 14(1): 11705.

Kipling, J.J. (2013). Adsorption from Solutions of Non-electrolytes. Academic Press.

Kurita, K. (1998). Chemistry and application of chitin and chitosan. Polymer Degradation and stability, 59(1-3): 117-120.

Labied, R.; Benturki, O.; Eddine Hamitouche, A.Y. and Donnot, A. (2018). Adsorption of hexavalent chromium by activated carbon obtained from a waste

lignocellulosic material (Ziziphus jujuba cores): Kinetic, equilibrium, and thermodynamic study. Adsorption science and technology, 36(3-4): 1066-1099.

Las-Casas, B.; Dias, I.K.; Yupanqui-Mendoza, S.L.; Pereira, B.; Costa, G.R.; Rojas, O.J. and Arantes, V. (2023). The emergence of hybrid cellulose nanomaterials as promising biomaterials. International Journal of Biological Macromolecules, 250: 126007.

Li Min, L.M.; Cui Wei, C.W.; Peng Xi, P.X.; Bai CaiMin, B.C. and Cui HengMin, C.H. (2009). Effect of dietary high copper on the oxidization in brain tissue of chickens. Chinese Journal of Veterinary Science, 29(10): 1334-1337.

Lu, G.; Yao, X.; Wu, X. and Zhan, T. (2001). Determination of the total iron by chitosan-modified glassy carbon electrode. Microchemical journal, 69(1): 81-87.

Mendizábal, E.; Ríos-Donato, N.; Ventura-Muñoz, M.G.; Hernández-Montelongo, R. and Verduzco-Navarro, I.P. (2024). Use of Chitosan–Iron Oxide Gels for the Removal of Cd2+ Ions from Aqueous Solutions. Gels, 10(10): 630.

Mohammed, I.; Al Shehri, D.; Mahmoud, M.; Kamal, M.S. and Alade, O.S. (2021). Impact of iron minerals in promoting wettability alterations in reservoir formations. ACS omega, 6(5): 4022-4033.

Mukherjee, M. (2006). Investigation of antifouling and disinfection potential of chitosan-coated iron oxide PAN hollow fiber membrane using Gram-positive and Gram-negative bacteria. Materials Science and Engineering: C, 26(5): 133–148.

Onsøyen, E., and Skaugrud, O. (1990). Metal recovery using chitosan. Journal of chemical technology and biotechnology (Oxford, Oxfordshire: 1986), 49(4): 395-404.

Park, J.V.; Park, D.M. and Park, K.K. (1986). Biomedical applications of chitin and chitosan. Polymer, 10: 641.

pérez, E.; Márquez, G. and Sagredo, V. (2019). Effect of calcination on characteristics of nickel ferrite nanoparticles synthesized by sol–gel method. Iraqi Journal of Applied Physics, 15(1): 13–17.

Radwan, M.A.; Al-Sweasy, O.H. and Elazab, H.A. (2017). Preparation of hydrogel based on acryl amide and investigation of different factors affecting rate and amount of absorbed water. Agricultural Sciences, 8(02): 161.

Shahidi, F. and Synowiecki, J. (1991). Isolation and characterization of nutrients and value-added products from snow crab (*Chionoecetes opilio*) and shrimp (*Pandalus borealis*) processing discards. Journal of agricultural and food chemistry, 39(8): 1527-1532.

Shallari, S.; Schwartz, C.; Hasko, A. and Morel, J.L. (1998). Heavy metals in soils and plants of serpentine and industrial sites of Albania. Science of the total environment, 209(2-3): 133-142.

Toan, N.V. (2009). Study on chitosan extraction from shrimp shell waste and its application in water treatment (Master's thesis). Ho Chi Minh City University of Technology, Ho Chi Minh City, Vietnam.

Vakili, M.; Deng, S.; Cagnetta, G.; Wang, W.; Meng, P.; Liu, D. and Yu, G. (2019). Regeneration of chitosan-based adsorbents used in heavy metal adsorption: A review. Separation and Purification Technology, 224: 373-387.

Wai, K.M.; Mar, O.; Kosaka, S.; Umemura, M. and Watanabe, C. (2017). Prenatal heavy metal exposure and adverse birth outcomes in Myanmar: a birth-cohort study. International journal of environmental research and public health, 14(11): 1339.

Yahya, M.D.; Obayomi, K.S.; Abdulkadir, M.B.; Iyaka, Y.A. and Olugbenga, A.G. (2020). Characterization of cobalt ferrite-supported activated carbon for removal of chromium and lead ions from tannery wastewater via adsorption equilibrium. Water Science and Engineering, 13(3): 202-213.

Yang, L.; Guo, C.; Jia, L.; Xie, K.; Shou, Q. and Liu, H. (2010). Fabrication of biocompatible temperature-and pH-responsive magnetic nanoparticles and their reversible agglomeration in aqueous milieu. Industrial and engineering chemistry research, 49(18): 8518-8525.

Zargar, V.; Asghari, M. and Dashti, A. (2015). A review on chitin and chitosan polymers: structure, chemistry, solubility, derivatives, and applications. ChemBioEng reviews, 2(3): 204-226.

Zhang, S. and Hu, X. (2003). Techniques and equipment for environmental pollution control. Techniques and Equipment for Environmental Pollution Control, 4(11): 68–71.

Zhao Li, Z.L.; Cui HengMin, C.H.; Yang Fan, Y.F.; Peng Xi, P.X. and Deng JunLiang, D.J. (2008). Effects of high dietary copper on hepatic oxidation and hepatocyte apoptosis in ducklings. Chinese Veterinary Science, 38(1):54-58.